

Your article (103-6711) from Magnetic Resonance in Medicine is available for download

=====

Magnetic Resonance in Medicine Published by John Wiley & Sons, Inc.

Dear Author,

Your article page proofs for Magnetic Resonance in Medicine are ready for review. John Wiley & Sons has made this article available to you online for faster, more efficient editing. Please follow the instructions below and you will be able to access a PDF version of your article as well as relevant accompanying paperwork.

First, make sure you have a copy of Adobe Acrobat Reader software to read these files. This is free software and is available for user downloading at <http://www.adobe.com/products/acrobat/readstep.html>.

Open your web browser, and enter the following web address:
<http://rapidproof.cadmus.com/RapidProof/retrieval/index.jsp>

You will be prompted to log in, and asked for a password. Your login name will be your email address, and your password will be ----

Example:

Login: your e-mail address

Password: ----

The site contains one file, containing:

- Author Instructions Checklist
- Adobe Acrobat Users - NOTES tool sheet
- Reprint Order form
- A copy of your page proofs for your article

Print out this file, and fill out the forms by hand. (If you do not wish to order reprints, please mark a "0" on the reprint order form.) Read your page proofs carefully and:

- indicate changes or corrections in the margin of the page proofs
- answer all queries (footnotes A,B,C, etc.) on the last page of the PDF proof
- proofread any tables and equations carefully
- check your figure legends for accuracy

Within 48 hours, please return via fax or express mail all materials to the address given below. This will include:

- 1) Page proofs with corrections
- 2) Reprint Order form

Return to:

Andrea Ritola
Senior Production Editor
John Wiley & Sons, Inc.

111 River Street, Hoboken, NJ 07030

Phone: 201-748-6550

Fax: 201-748-6281/6182

Technical problems? If you experience technical problems downloading your file or any other problem with the website listed above, please contact Doug Frank (e-mail: frankd@cadmus.com, phone: 800-238-3814 x615) or 717-721-2615.

Questions regarding your article? Please don't hesitate to contact me with any questions about the article itself, or if you have trouble interpreting any of the questions listed at the end of your file. **REMEMBER TO INCLUDE YOUR ARTICLE NO. (103-6711) WITH ALL CORRESPONDENCE.** This will help both of us address your query most efficiently.

As this e-proofing system was designed to make the publishing process easier for everyone, we welcome any and all feedback. Thanks for participating in our e-proofing system!

This e-proof is to be used only for the purpose of returning corrections to the publisher.

Sincerely,

Andrea Ritola
Senior Production Editor
John Wiley & Sons, Inc.
111 River Street, Hoboken, NJ 07030

Phone: 201-748-6550

Fax: 201-748-6281/6182



WILEY

Publishers Since 1807

111 RIVER STREET, HOBOKEN, NJ 07030

MAGNETIC RESONANCE IN MEDICINE PRODUCTION

*****IMMEDIATE RESPONSE REQUIRED*****

Please follow these instructions to avoid delay of publication.

READ PROOFS CAREFULLY

- This will be your only chance to review these proofs.
- Please note that the volume and page numbers shown on the proofs are for position only.

ANSWER ALL QUERIES ON PROOFS (Queries for you to answer are attached as the last page of your proof.)

- Mark all corrections directly on the proofs. Note that excessive author alterations may ultimately result in delay of publication and extra costs may be charged to you.

CHECK FIGURES AND TABLES CAREFULLY

- Check size, numbering, and orientation of figures.
- All images in the PDF are downsampled (reduced to lower resolution and file size) to facilitate Internet delivery. These images will appear at higher resolution and sharpness in the printed article.

COMPLETE REPRINT ORDER FORM

- Fill out the attached reprint order form. It is important to return the form even if you are not ordering reprints. Reprints will be shipped 4-6 weeks after your article appears in print.

ADDITIONAL COPIES

- If you wish to purchase additional copies of the journal in which your article appears, please contact Jill Gottlieb at (201) 748-8839, fax (201) 748-6021, or E-mail at jgottlieb@wiley.com

RETURN WITHIN 48 HOURS OF RECEIPT VIA FAX TO

201-748-6182/6281

or direct questions to:

Andrea Ritola, Senior Production Editor

Magnetic Resonance in Medicine

Phone: 201-748-6550

Refer to journal acronym (MRM) and article production number

Softproofing for advanced Adobe Acrobat Users - NOTES tool

NOTE: ADOBE READER FROM THE INTERNET DOES NOT CONTAIN THE NOTES TOOL USED IN THIS PROCEDURE.

Acrobat annotation tools can be very useful for indicating changes to the PDF proof of your article. By using Acrobat annotation tools, a full digital pathway can be maintained for your page proofs.

The NOTES annotation tool can be used with either Adobe Acrobat 3.0x or Adobe Acrobat 4.0. Other annotation tools are also available in Acrobat 4.0, but this instruction sheet will concentrate on how to use the NOTES tool. Acrobat Reader, the free Internet download software from Adobe, DOES NOT contain the NOTES tool. In order to softproof using the NOTES tool you must have the full software suite Adobe Acrobat Exchange 3.0x or Adobe Acrobat 4.0 installed on your computer.

Steps for Softproofing using Adobe Acrobat NOTES tool:

1. Open the PDF page proof of your article using either Adobe Acrobat Exchange 3.0x or Adobe Acrobat 4.0. Proof your article on-screen or print a copy for markup of changes.
2. Go to File/Preferences/Annotations (in Acrobat 4.0) or File/Preferences/Notes (in Acrobat 3.0) and enter your name into the "default user" or "author" field. Also, set the font size at 9 or 10 point.
3. When you have decided on the corrections to your article, select the NOTES tool from the Acrobat toolbox and click in the margin next to the text to be changed.
4. Enter your corrections into the NOTES text box window. Be sure to clearly indicate where the correction is to be placed and what text it will effect. If necessary to avoid confusion, you can use your TEXT SELECTION tool to copy the text to be corrected and paste it into the NOTES text box window. At this point, you can type the corrections directly into the NOTES text box window. **DO NOT correct the text by typing directly on the PDF page.**
5. Go through your entire article using the NOTES tool as described in Step 4.
6. When you have completed the corrections to your article, go to File/Export/Annotations (in Acrobat 4.0) or File/Export/Notes (in Acrobat 3.0). Save your NOTES file to a place on your harddrive where you can easily locate it. **Name your NOTES file with the article number assigned to your article in the original softproofing e-mail message.**
7. **When closing your article PDF be sure NOT to save changes to original file.**
8. To make changes to a NOTES file you have exported, simply re-open the original PDF proof file, go to File/Import/Notes and import the NOTES file you saved. Make changes and re-export NOTES file keeping the same file name.
9. When complete, attach your NOTES file to a reply e-mail message. Be sure to include your name, the date, and the title of the journal your article will be printed in.



REPRINT BILLING DEPARTMENT 111 RIVER STREET HOBOKEN, NJ 07030

PHONE: (201) 748-8789; FAX: (201) 748-6326

E-MAIL: reprints@wiley.com

PREPUBLICATION REPRINT ORDER FORM

Please complete this form even if you are not ordering reprints. This form **MUST** be returned with your corrected proofs and original manuscript. Your reprints will be shipped approximately 4 weeks after publication. Reprints ordered after printing will be substantially more expensive.

JOURNAL Magnetic Resonance in Medicine VOLUME _____ ISSUE _____

TITLE OF MANUSCRIPT _____

MS. NO. MRM _____ NO. OF PAGES _____ AUTHOR(S) _____

No. of Pages	100 Reprints	200 Reprints	300 Reprints	400 Reprints	500 Reprints
	\$	\$	\$	\$	\$
1-4	336	501	694	890	1052
5-8	469	703	987	1251	1477
9-12	594	923	1234	1565	1850
13-16	714	1156	1527	1901	2273
17-20	794	1340	1775	2212	2648
21-24	911	1529	2031	2536	3037
25-28	1004	1707	2267	2828	3388
29-32	1108	1894	2515	3135	3755
33-36	1219	2092	2773	3456	4143
37-40	1329	2290	3033	3776	4528

**REPRINTS ARE ONLY AVAILABLE IN LOTS OF 100. IF YOU WISH TO ORDER MORE THAN 500 REPRINTS, PLEASE CONTACT OUR REPRINTS DEPARTMENT AT (201) 748-8789 FOR A PRICE QUOTE.

Please send me _____ reprints of the above article at \$ _____

Please add appropriate State and Local Tax (Tax Exempt No. _____) \$ _____
for United States orders only.

Please add 5% Postage and Handling \$ _____

TOTAL AMOUNT OF ORDER** \$ _____

***International orders must be paid in currency and drawn on a U.S. bank*

Please check one: Check enclosed Bill me Credit Card
If credit card order, charge to: American Express Visa MasterCard

Credit Card No _____ Signature _____ Exp. Date _____

BILL TO: Name _____ **SHIP TO:** (Please, no P.O. Box numbers) Name _____
Institution _____ Institution _____
Address _____ Address _____

Purchase Order No. _____ Phone _____ Fax _____
E-mail _____



WILEY

Publishers Since 1807

MAGNETIC RESONANCE IN MEDICINE (MRM)

To: Andrea Ritola

Senior Production Editor

Phone: 201-748-6550

Fax: 201-748-6281/6182

From: _____

Date: _____

Pages including
this cover page: _____

re:

Retrospective Coregistration of Functional Magnetic Resonance Imaging Data Using External Monitoring

Marleine Tremblay,¹ Fred Tam,² and Simon J. Graham^{1,2,3*}

Coregistration is essential for correcting head motion artifacts in functional magnetic resonance imaging (fMRI). Coregistration algorithms typically realign images through optimization of a similarity measure based on voxel signal intensities. However, coregistration can also be performed through external monitoring, whereby a tracking device measures head motion directly and independently of the imaging data. This paper describes development of external monitoring using fMRI-compatible infrared cameras. Three subjects participated in block-design fMRI experiments consisting of bilateral finger tapping alone and tapping combined with visuomotor tracking to produce controlled task-correlated head motion. Functional MRI time-series were coregistered using the external monitoring technique and a known image-based algorithm for comparison. Over various performance characteristics, external monitoring and image-based coregistration exhibited good agreement, in particular reducing signals correlated with millimeter task-correlated motions by 50–100%, with a 5% difference between the two techniques. These results promise future applications and refinements of external monitoring in patient populations where head motion is especially problematic. Possibilities include 3D prospective coregistration during real-time fMRI, coregistration of individual slices, and motion correction in anatomic MRI. Magn Reson Med 53:000–000, 2005. © 2005 Wiley-Liss, Inc.

Key words: fMRI; head motion; image coregistration; position tracking; fMRI-compatible devices

Head motion is a fundamental problem in functional magnetic resonance imaging (fMRI). The problem arises because millimeter head movements, relative to the spatial coordinate frame of the images, are sufficient to cause voxel signal intensity changes that appear very similar to the blood oxygen level dependent (BOLD) signals that reflect neuronal activity (1). Two distinct types of motion are problematic: random motion increases the effective noise level and tends to decrease the total number of activated voxels that are detected, whereas task-correlated motion (TCM) occurs synchronously with alternating task and rest conditions, introducing artifacts that masquerade

as increased brain activation and that may be particularly severe in patients with impaired brain function (2).

In combination with fast imaging techniques (e.g., echo planar or spiral *k*-space readouts), retrospective coregistration methods are key to reducing head motion effects and are used to realign the time-series data to a reference image collected during the fMRI session (3–5). Conventional retrospective coregistration uses rigid-body (or affine) transformation consisting of six (or more) realignment parameters. Realignment parameters are typically estimated by optimizing a similarity measure based on voxel signal intensity values, quantifying the difference between a specific image in the time-series, and the reference. Prospective coregistration is also being developed to adjust scanning to track with moving anatomy, requiring fast methods to measure head motion (6–10), although retrospective coregistration currently predominates fMRI research and is the principal focus of this work.

Although retrospective coregistration is effective, limitations are evident. Poor spatial resolution, signal- and contrast-to-noise ratio, and image artifacts may deteriorate coregistration accuracy. Most coregistration algorithms correct only for small movements (translations of 1–2 voxels and rotations of 1–2°) and may be less reliable at larger amplitudes. Last, head motion is sampled at the imaging repetition time (TR), providing only one set of realignment parameters per stack of multislice images, with the assumption of no interslice motion.

A promising alternative is to perform coregistration using external monitoring, using a tracking device (TD) independent of the MR imaging process and data. This offers the possibility of sampling head motion at higher temporal resolution and with improved accuracy. This paper describes development of external monitoring using an infrared tracking device for retrospective 3D coregistration of fMRI data. Performance of the technique is carefully assessed for both random motion and TCM and compared with coregistration achieved by widely used fMRI data processing software (Analysis of Functional NeuroImages, AFNI (11,12)). The comparison is not intended to assess the merits of using the TD versus image-based retrospective coregistration generally, but rather to confirm proof-of-concept for the external monitoring.

METHODS

Experimental Setup, Preliminary Characterization

Figure 1 illustrates the experimental setup. The TD (Polaris, model P4 Position sensor, enhanced ElectroMagnetic Interference option, Northern Digital, Inc., Waterloo, Canada) was mounted on a wooden frame facing the bore of an MRI system operating at 1.5 T (Signa CV/i configuration, LX 8.4, GE Medical Systems, Waukesha, WI). The TD uses

¹Department of Medical Biophysics, University of Toronto, Toronto, Canada.

²Imaging Research, Sunnybrook and Women's College Health Sciences Centre, Toronto, Canada.

³Rotman Research Institute, Baycrest Centre for Geriatric Care, Toronto, Canada.

Contract grant sponsor: Canadian Institutes of Health Research (CIHR); Contract grant sponsor: General Electric Medical Systems Canada; Contract grant sponsor: Natural Sciences and Engineering Research Council (NSERC); Contract grant sponsor (to M. T.): Fonds de Recherche sur la Nature et les Technologies (FCAR) of Quebec, Canada.

*Correspondence to: S. J. Graham, S650, Imaging Research, Sunnybrook & Women's College Health Sciences Centre, 2075 Bayview Avenue, Toronto, Ontario M4N 3M5, Canada. E-mail: simon.graham@sw.ca

Received 6 November 2003; revised 23 July 2004; accepted 12 August 2004.

DOI 10.1002/mrm.20319

Published online in Wiley InterScience (www.interscience.wiley.com).

© 2005 Wiley-Liss, Inc.

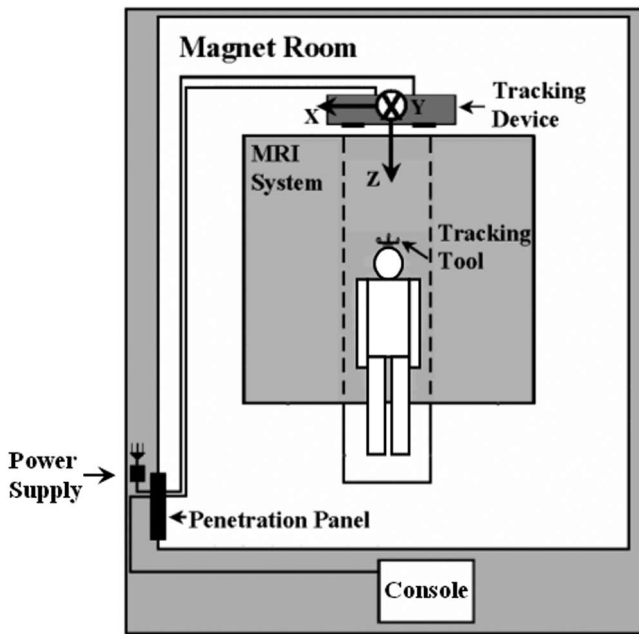


FIG. 1. Experimental setup in magnet room (top view, not to scale).

two independent charge-coupled devices (CCDs) to detect infrared light reflected in its direction. Surrounding the lens of each CCD is an array of infrared emitting diodes to illuminate the field of view. Functional MRI compatibility was achieved by relocating the power supply from inside the TD main unit to outside of the magnet room, using shielded cables routed through the filtered penetration panel.

Using parallax calculations, the TD tracks plastic tools with precisely defined spatial arrangements of three or four rigidly fixed, reflective markers (Traxtal Technologies, Inc., Toronto, Canada) (13). The set of detected positions on a given tool is compared with information preloaded in the TD about the theoretical marker positions. A least squares fit of the two sets of positions determines the spatial transformation that must be applied to match the two sets (position and orientation data with 6 degrees of freedom, 6DOF) which is transmitted via serial communication to a computer console. Position measurements were acquired at a rate of 4.8 Hz, considerably exceeding that required for image-based coreg-

istration of fMRI time-series (e.g., 0.5 Hz for a TR of 2 sec, assuming single-shot imaging).

To test the accuracy of the TD, repeated position measurements were taken at precise locations within the magnet. The TD translation accuracy along each axis was taken to be the smallest displacement that could be applied to the tracking tool along that axis such that the slope of linear fit between applied and measured displacement was 1.00 ± 0.01 . Translation accuracies in x, y, and z of 0.01 mm, 0.03, and 0.1 mm, respectively, were obtained over a 2-cm-diameter spherical volume with the axes pointing as illustrated in Fig. 1. Angular accuracies in roll, pitch, and yaw of 0.009° , 0.23° , and 0.23° were obtained, respectively, by applying rotations to the tracking tool with a stepper motor (Model No. QM-57-83, Parker Hannifin Corp., Rohnert Park, CA). These accuracies were judged sufficient to consider using the TD to coregister fMRI data.

The stability of TD measurements was assessed by tracking a stationary tool for several hours. Radial linear drift rates ($\sqrt{(dx/dt)^2 + (dy/dt)^2 + (dz/dt)^2}$) of 1.2 mm/hr were observed during the first 45 min after power-up, presumably due to temperature variation within the TD electronics. To improve stability, the TD was warmed up for 60 min prior to use, and not one but two tools were tracked during fMRI (Fig. 2). The tracking tool was strapped to the subject's head using a small cap composed of two elastic bands surrounding the forehead, without a chin strap to avoid tool motion during swallowing. Foam padding was inserted between the tool and the head to avoid slight magnetic susceptibility artifacts during fMRI due to proximity of the tracking tool to the brain surface. A reference tool was mounted on the stationary head coil. Because the TD data for both tools drifted similarly, stability of the tracking tool information was increased by calculating the reference tool's linear drift rates along the three orthogonal axes and subtracting these linear trends from the tracking tool data. The subsequent radial drift rate was reduced approximately 10-fold (0.1 ± 0.03 mm/hr). Linear drifts in angular position were similarly attenuated about all three orthogonal axes.

Calibration and TD Data Processing

A calibration procedure was developed to estimate the transformation matrix to convert head motion information

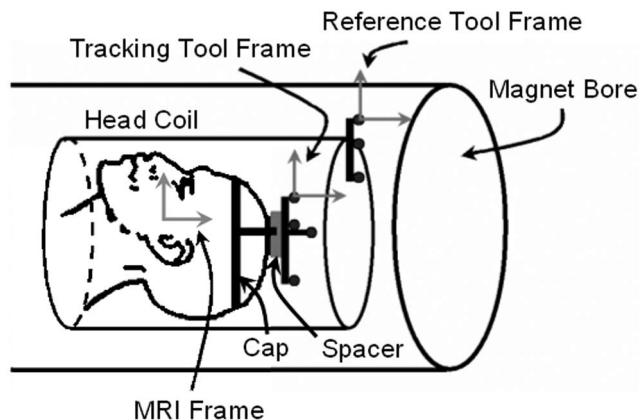


FIG. 2. Experimental setup within magnet bore (side view, not to scale).

from the TD coordinate frame to the coordinate frame of the MRI system to enable image coregistration about magnet isocenter. If the coordinates of at least three points are measured in two different Cartesian frames, in theory the transformation between the frames can be obtained. Seven holes (2.5 mm depth, 2.5 mm diameter) were drilled in the tracking tool at precise locations and filled with aqueous agar solution containing approximately 1 mmol/liter of contrast agent (Gd-DTPA, Omniscan, Nycomed) to make the tool visible by MRI. The distance of each hole center relative to the origin of the spatial coordinate frame of the tracking tool was provided by the manufacturer.

The 6DOF reported by the TD actually corresponds to measurement of the specific tool frame relative to the TD frame (Fig. 2). Given the 3D position of a hole in the tracking tool frame, r_o , the 3D position of the tool frame in the TD frame, r_{Tool} , and R , a 3×3 matrix representing the 3D orientation of the tool frame relative to the TD frame, the 3D position of the hole can be calculated in the TD frame, r_{TD} :

$$r_{TD} = Rr_{Tool} + r_o. \quad [1]$$

In addition, the 3D position of the same hole in the MRI frame, r_{MRI} , is readily obtained from a high-resolution MR image of the tracking tool. The transformation of positions in the TD frame to the MRI frame was estimated via Horn's closed-form solution (14), which is time-efficient (fast) and holds for an arbitrary number of points (greater than 3) measured in both frames. The latter issue is important because the positions measured by the TD and by MRI have experimental uncertainty, and the transformation can be estimated more accurately by including more points. The transformation was subsequently applied to the negative of the head motion parameters to achieve the appropriate realignment parameters.

Rather than developing coregistration software in its entirety, TD realignment parameters were incorporated into the spatial interpolation module in AFNI, enabling direct comparison with image coregistration performed using AFNI alone. All other aspects of the data processing were kept identical in the comparison, ensuring that differences in the resulting activation images could be attributed solely to differences in estimating head motion.

The TD was controlled using C++ software developed in the laboratory and executed on a laptop computer (Toshiba 4020CDT, 300 MHz Pentium II CPU, 96 MB RAM, Windows 98 operating system). TD data acquisition was synchronized with fMRI time-series data collection using a trigger pulse sent by the laptop. The TD motion data were also processed slightly prior to calculating realignment parameters. A third order, one-dimensional median filter (the median of each datum and its nearest neighbors in time) was applied to remove a small amount of spike noise that was observed qualitatively, while preserving the sharpness of motion trends. In addition, the TD motion parameters were resampled by spline interpolation to the exact end of the n th TR interval (or equivalently, the first set of motion parameters of the $(n + 1)$ th TR interval) for 3D coregistration of the $(n + 1)$ th stack of multislice images. This ensured that there were as many sets of

motion parameters as stacks of multislice images in the associated fMRI time series, enabling 3D coregistration assuming rigid-body motion.

FMRI Tasks

Two behavioral tasks were performed in block designs with alternating "task" and "rest" conditions of 20-sec duration. The first task involved self-paced bilateral tapping of alternating fingers. As this task was performed on a small group of young, healthy adults (see below), predominantly random head motion was anticipated. The second task was designed explicitly to include well-controlled TCM, requiring the same bilateral finger tapping in the presence of a visuomotor tracking task in which the subject followed a moving object based on a visual representation of his or her head position. Visual stimuli were displayed on a back-projection screen at the entrance to the magnet bore using an LCD projector (Revolution III, Boxlight 6000, Boxlight Corp.) and viewed by the subject using angled mirrors in the MRI system's quadrature bird-cage head coil. An open "target" circle, initially positioned in the center of the screen, moved alternately from side to side at the rate of one cycle per 20 sec along a path of length λ . The amount of TCM associated with the task was then controlled by varying λ . Note that the entire length of the horizontal path on the projected display was fixed; rather, a scaling factor was varied between the path length of the display and the actual head motion. In what follows, λ represents head motion in millimeters.

Head motion was measured by the TD and was represented visually in the form of a black disk under control of the subject, who was to keep the disk centered inside the target circle by moving his or her head appropriately (primarily roll rotation). They were also asked to perform this task while fixating foveally and while performing bilateral finger tapping. During the rest condition, subjects fixated while the target circle and the disk moved from side to side in lock step for one cycle (i.e., visual stimuli were similar during task and rest periods). The initial direction of target motion was alternated for each task period.

In addition to assessing the ability of the TD to correct for both random motion and TCM, the tracking task was expected to involve elements of the vestibular system involved in detecting head movement and generation of compensatory eye movements (15). Detailed analysis and interpretation of the associated brain activity is beyond the methodological scope of this work.

Subjects

Three young, healthy subjects (right-handed males, average age 25 years, range 24–27 years old) volunteered for this study under approval of the Research Ethics Board at Sunnybrook & Women's College Health Sciences Centre. All gave informed consent and completed the simple bilateral finger tapping experiment. The TCM was varied in the tracking experiments, however, and subjects were given different path lengths, λ , ranging from 1 to 12 mm (Table 1). Data for subject 1 with $\lambda = 2$ mm were discarded because the tracking tool was mounted improperly.

Table 1
Number of Trials per Tracking Path Length λ

λ (mm)	No. Trials		
	Subject 1	Subject 2	Subject 3
0	2	6	2
1	2	3	1
2	1*	2	1
6	0	2	1
12	0	2	0

*Not included in subsequent analysis. Tracking tool was mounted improperly.

Imaging and Postprocessing

Functional MRI data were acquired using single-shot spiral readout (TE/TR/2 = 40 msec/2000 msec/80°, field of view (FOV) = 20 cm, slice thickness = 5 mm, matrix = 64 × 64, 17–19 slices) (16). Anatomic images were acquired with 3D fast spoiled gradient echo imaging (TE/TR/2 = 6 msec/35 msec/35°, FOV = 22 cm, slice thickness = 1.4 mm, matrix = 256 × 128, 124 slices). Calibration images of the tracking tool were acquired similarly but with higher spatial resolution (slice thickness = 0.7 mm, matrix 512 × 512). After off-line reconstruction of the spiral k -space data, including gridding and correction for magnetic field inhomogeneity and Maxwell gradient effects (17), all subsequent data postprocessing was performed within AFNI. For each fMRI experiment, two time series data sets were created using Fourier interpolation, in addition to the original, uncoregistered data. One data set was coregistered using AFNI realignment parameters and the other using TD realignment parameters. All other processing, which included linear and quadratic detrending, spatial smoothing (Gaussian filter with 4 mm FWHM), temporal smoothing (3 point median filter), boxcar correlation analysis, and masking fMRI signals to zero outside of the brain, was performed identically. The voxel-wise statistical threshold for each brain activation image was $P = 3.4 \times 10^{-7}$ ($P = 0.01$, Bonferroni corrected) with a threshold correlation coefficient (CC_{TH}) of 0.39.

Analyses

For each fMRI experiment, the coregistration results obtained with AFNI alone and with AFNI using TD realignment parameters were compared various ways. The time series of six realignment parameters estimated by AFNI and the TD was plotted for comparison. Brain activation

images were compared both qualitatively by visual inspection and quantitatively by plotting the number of detected activated brain voxels as a function of BOLD percent signal change (an “activation histogram”). Each activation histogram was plotted with 101 bins. In the fMRI experiments involving visuomotor tracking, TCM was still present to some degree in voxels along the brain periphery even after coregistration, suggesting comparison of the ability of the two coregistration methods to attenuate signal variations due to TCM. This was quantified by calculating the voxel-wise correlation with the roll rotation waveform measured by the TD during the fMRI experiment of interest. The number of voxels significantly correlated with roll rotation (for the same P and CC_{TH} values given above) was plotted as a function of roll correlation coefficient in a “TCM histogram” containing 101 bins over the full range of possible correlation values (−1.0–1.0). Both the activation and the TCM histogram approaches were undertaken for the uncoregistered time-series data as well.

RESULTS

Bilateral Finger Tapping Experiments

The six realignment parameters for a representative bilateral finger tapping experiment are shown in Fig. 3, in which the AFNI results from image-based coregistration and the TD results are plotted as a function of time. There is good agreement between the two coregistration techniques, although the TD results show more high frequency fluctuations. Figure 4A shows representative examples of the associated activation images obtained after coregistration. The images obtained solely using AFNI (left) and those obtained using TD data (right) are very similar, depicting activation of the two primary sensorimotor cortices, left parietal cortex, and the supplementary motor area. The two coregistrations also agree well when comparing the activation histograms for the whole brain (Fig. 4B), allowing detection of very similar numbers of activated voxels for each given value of BOLD percent signal change, positive and negative.

Bilateral Finger Tapping and Tracking Experiments

Figure 5 shows AFNI and TD realignment parameters for a representative visuomotor tracking experiment ($\lambda = 1$ mm). As anticipated, visuomotor tracking is observed primarily as roll rotation, with some x translation. Good agreement is observed between the two sets of realignment

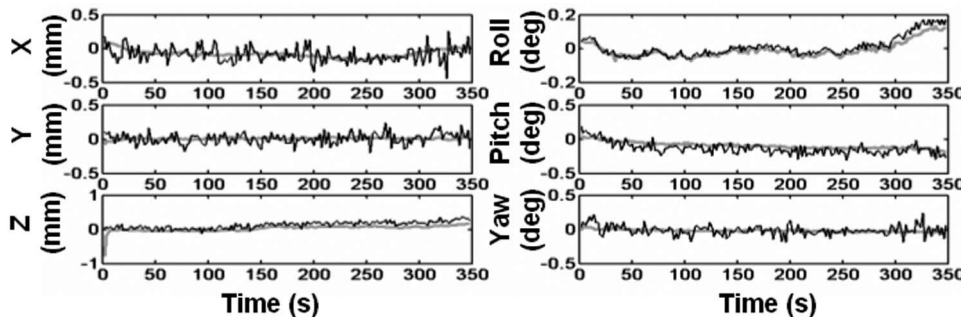


FIG. 3. Realignment parameters for a representative bilateral finger tapping experiment. Results from image-based coregistration in AFNI (gray line) and those from the TD (black line) exhibit very consistent trends. The TD parameters show more rapid temporal fluctuations.

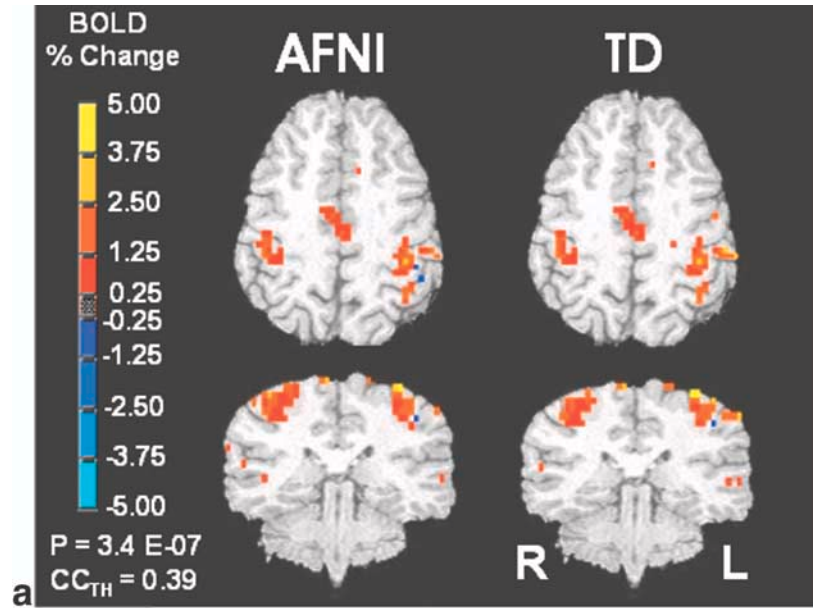


FIG. 4. (a) Activation images obtained using AFNI exclusively (left) and using the TD data (right) for a representative subject performing bilateral finger tapping. (b) “Activation histograms” illustrating the number of active voxels detected as a function of BOLD signal (AFNI: gray line; TD: black line). In both (a) and (b) the two sets of activation data are in good agreement.

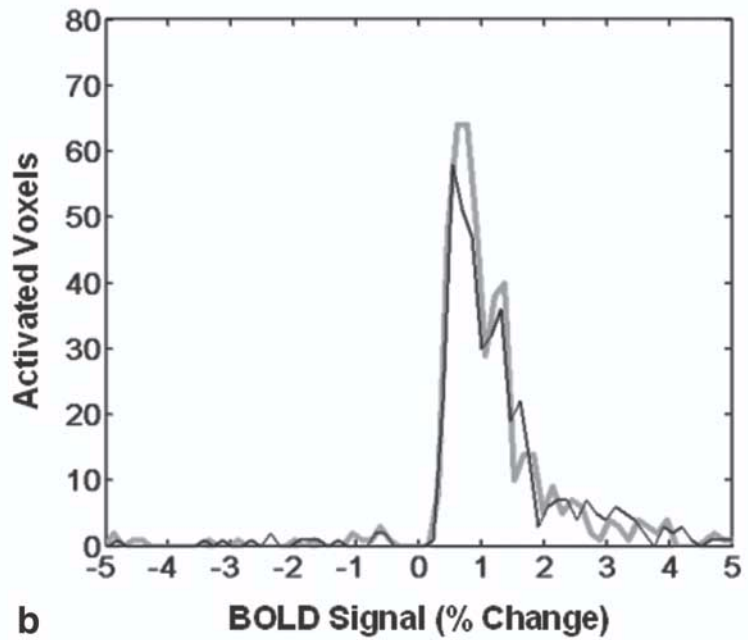
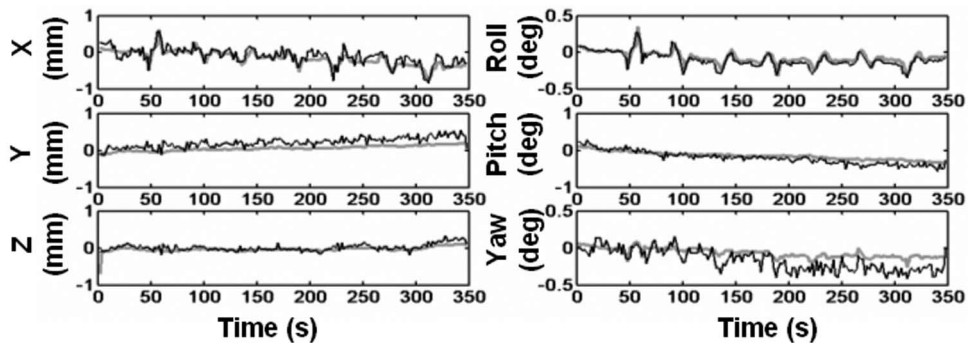


FIG. 5. Realignment parameters for a representative bilateral finger tapping and tracking task ($\lambda = 1$ mm; AFNI, gray line; TD, black line). Results for both coregistration techniques are very similar, although TD data again show more rapid fluctuations. Slightly more systematic deviation between the techniques is also observable compared to the results shown.



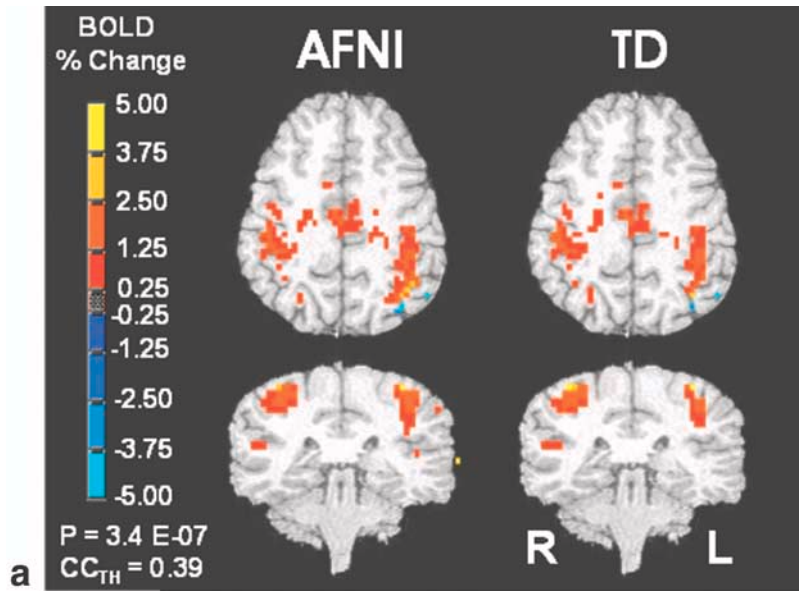
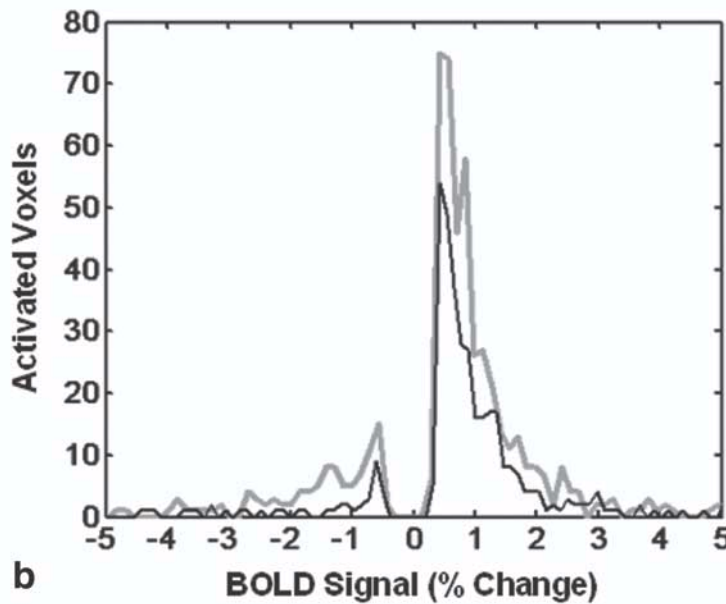


FIG. 6. (a) Activation images obtained solely using AFNI (left) and using the TD data (right) for a representative subject performing bilateral finger tapping and tracking ($\lambda = 1$ mm). (b) Associated activation histograms for the whole brain (AFNI, gray line; TD, black line). For this subject, more active voxels were obtained using AFNI alone.



parameters, with the TD data exhibiting more high-frequency fluctuations, although there are slightly more deviations than observed in Fig. 3. The associated representative activation images and activation histograms (Fig. 6) are consistent with these observations. Both sets of activation images (Fig. 6A) show more extensive brain activity than that observed for tapping alone (Fig. 4A), due to the demands of visuomotor tracking. The activation histograms (Fig. 6B) show for this subject that external monitoring results in slightly fewer activated voxels throughout the brain, compared to what can be obtained solely by AFNI. Compared to no coregistration, both coregistration methods reduce the number of significant roll-correlated voxels by approximately 10-fold (data not shown).

Results for All Three Subjects

Voxel counts versus λ are shown in Fig. 7 for all three subjects. Experiments involving bilateral finger tapping

alone are plotted as $\lambda = 0$ mm and, as mentioned above, increased voxel counts are expected for the visuomotor tracking task ($\lambda > 0$ mm). In Fig. 7a, all three analyses report similar voxel counts for $\lambda = 0$ mm, as expressed by the mean plus or minus half the range of the data (uncoregistered: 340 ± 430 ; AFNI: 320 ± 300 ; TD: 260 ± 240). This also holds for $\lambda = 1-6$ mm, although more voxels were activated (uncoregistered: 970 ± 1200 ; AFNI: 1000 ± 1200 ; TD: 780 ± 1000). For the two coregistration techniques over this range of λ , a repeated-measures two-way ANOVA indicates no statistically differences (main effect of coregistration method: $F(1,1) = 2.85$, ns; main effect of λ : $F(3,3) = 1.51$, ns). Visual inspection of Fig. 7a suggests a possible, slight trend for the TD to detect less activated voxels. For $\lambda = 6-12$ mm, a very large increase voxel counts is observed irrespective of the analysis method and is very likely spurious.

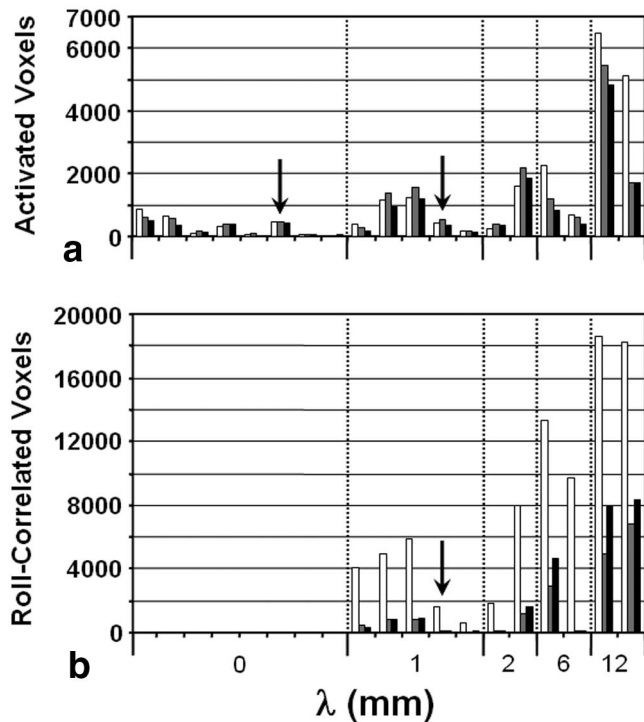


FIG. 7. Bar plots of voxel count versus λ for all validation experiments (no coregistration, white; AFNI alone, gray; TD, black). Bilateral finger tapping without tracking is represented by $\lambda = 0$. Arrows indicate data for representative subjects shown in the previous figures. Although (a) the number of activated voxels agrees well for the three techniques, (b) the number of roll-correlated voxels is significantly higher when coregistration is not performed. AFNI and TD data remain quite similar throughout. There appears to be a trend that the TD results in slightly fewer activated voxels and slightly more roll-correlated voxels, although this is not statistically significant over the small number of subjects investigated. See text for further details.

Additionally for $\lambda > 0$ mm, there are significantly more roll-correlated voxels in the case of no coregistration (Fig. 7b) and these voxel counts correlate very strongly with λ ($R^2 = 0.9925$). In contrast, both coregistration techniques suppress the number of roll-correlated voxels for $\lambda = 1-6$ mm by 50–100% compared to when coregistration is not performed, with 5% difference in suppression between the two techniques. Figure 7 suggests overall that both coregistration techniques lead to the production of highly similar, robust activation images for $\lambda = 0-6$ mm.

DISCUSSION

There remains a strong need for improved coregistration with higher spatial accuracy and temporal resolution to expand fMRI applications. For example, higher spatial accuracy is required due to the continued development of high- and very-high-field MRI systems, which are beginning to resolve brain function at the level of columnar organization (18). Higher temporal resolution is required to measure the delay between BOLD signals in different brain regions on a time scale of 100 msec or less (19) or to coregister different regions (e.g., slices or shots) of a time

series (e.g., multislice or 3D data) separately to improve motion correction within the TR interval.

The development of MR-compatible tracking systems for improved coregistration is attractive, but challenging. There is a preliminary report of a TD designed to operate using laser signals (20), although the laser light must (i) strike appropriate reflectors located on the moving head and (ii) be detected robustly. Practically, both are difficult to achieve. Radiofrequency locator coils wrapped around MR-visible samples can be tracked based on resonance frequency using magnetic field gradients (8). However, such devices reduce the temporal resolution that is achievable during fMRI because interleaved MR experiments are required for position tracking. Gradient nonlinearities are also a source of inaccuracy, requiring accurate knowledge of the 3D field distribution for the gradient coils. The latter issue is important for other TD approaches (21) using the voltages induced in small coils during the time-varying gradients in an MRI pulse sequence. In this case, however, temporal sampling is inherently nonuniform.

In comparison, the external monitoring described here is relatively straightforward. The Polaris TD operates in the infrared spectrum, ensuring that fMRI experiments involving visual stimuli are possible. Line of sight is required and it is preferable to use a birdcage coil without an end cap and appropriate cable routing to ensure that the tracking and reference tools are not obscured. Although the plastic tracking tool is light and the cap fits snugly, some motion of the tracking tool relative to the brain is possible. Elastic motion might occur, but the scalp moving over the skull is likely more problematic and can be reduced by patient training.

Coregistration Involving AFNI Alone and Using the TD

Compared to coregistration using AFNI alone, the TD realignment parameters did exhibit more high-frequency fluctuations and slight systematic differences (Figs. 3 and 5). Possible sources for these effects are: (i) the patients themselves (e.g., TD measurements reflect true head motion not measured by AFNI) and (ii) the patient-specific experimental setup and methodology (e.g., the tracking tool requires better mounting on the head). These problems likely are not due to the camera/tracking tool combination per se, however, given that the intrinsic tracking error (see Methods) is considerably smaller than the noise fluctuations observed in Figs. 3 and 5.

The calibration procedure in this study used seven coplanar points and a manual procedure for determining the associated voxel locations within MR images. Future implementation could include more, noncoplanar points as well as automated image processing to determine the MRI coordinates of each point. In addition, a new tool could be designed such that the centroid of its spatial distribution of points, used to determine the calibration transformation, lies close to the geometric center of the relevant brain anatomy to be coregistered. Such modifications can reduce the error in a coordinate frame transformation calculated using a point-based approach (22). Furthermore, a rigid mount to provide accurate and repeatable positioning of the TD could potentially eliminate calibration before each fMRI session.

The representative image-based coregistration in the present work is also subject to several sources of error. For example, signal intensity changes that are inconsistent with rigid-body motion of the entire head include eye motion (23), the BOLD effect itself (24), and spatial distortion caused by movement of anatomy within the magnet bore (25). Indeed, the TD may have use in validating coregistration algorithms. With development of appropriately detailed phantoms under known motion and known patterns of artificial dynamic “activation,” such effects could be studied in detail.

A novel aspect of the present study was to perform fMRI using two behavioral tasks, one with predominantly random head motion (bilateral finger tapping) and one with predominantly TCM (bilateral finger tapping and visuomotor tracking). Importantly, the two tasks also exhibited slightly different patterns of brain activity. The visuomotor tracking task additionally involved bilateral medial frontal gyri and the right superior frontal gyrus (not shown in Fig. 6), regions associated with vestibular function (26). It is possible that this task and technology could be adapted specifically to visualize and improve understanding of vestibular functional neuroanatomy, beyond fMRI with traditional means of perturbing the vestibular system (e.g., galvanic stimulation (15)). Furthermore, Fig. 7 indicates that for λ less than approximately twice the voxel dimension (6 mm in-plane), the head motion introduced by the specific visuomotor tracking task does not adversely contaminate fMRI signals if retrospective coregistration is performed. Although it is typical to discard fMRI data containing head motions that corresponding to a fraction of the voxel size, Fig. 7 indicates that for well-controlled fMRI tasks and analyses such an approach may be overly conservative and tasks actually designed to involve small amounts of head motion can be contemplated.

Improving Coregistration

The brain is not a rigid body and deforms approximately 50–100 μm at the cortex due to blood flow, irrespective of head motion (27). Coregistration techniques can still be improved toward this fundamental limit, and external monitoring applications are one approach. Although the data in this study were acquired at 4.8 Hz, the data acquisition rate has now been improved to 30 Hz, half the hardware limit. Such high sampling enables coregistering different slices of a given volume individually, rather than assuming that all slices in a multislice acquisition are acquired simultaneously. An iterative “map-slice-to-volume” algorithm has shown improved sensitivity and localization of fMRI signals in comparison with conventional coregistration (28). Such corrections make the brain look “more rigid” and can be used with conventional 3D coregistration to correct for residual errors.

In addition, compared to use of navigator echoes (6), the high sampling rate of the TD facilitates prospective coregistration, potentially in combination with retrospective coregistration to reduce residual errors (10). Others are adopting infrared tracking technology toward similar goals (29).

The TD can also provide real-time visual feedback via a projector to subjects about their head motion during fMRI,

allowing them to compensate for small head movements immediately (30). Images of brain activity will potentially be influenced, however, by the fact that the fMRI signal baseline already engages brain regions involved in visuo-motor coordination. In real-time fMRI applications, rapid presentation of head motion information is also very useful to provide direct warning of poor data quality. More generally, potential applications include *k*-space motion corrections for diverse 2D or 3D MRI applications, coregistration in dynamic contrast-enhanced MRI, and tracking of probes and instruments to adjust the scanning plane during MRI-guided therapy. Obviously, there is considerable scope for future development.

ACKNOWLEDGMENTS

The authors thank Philippe C. Pontbriand for his assistance in various aspects of image processing, Nicole Baker for her help building various components of the experimental apparatus, Gordon Mosher (NDI) for important technical discussions, and Dr. Sofia Chavez for critically evaluating the manuscript.

REFERENCES

1. Ogawa S, Lee TM, Kay AR, Tank DW. Brain magnetic resonance imaging with contrast dependent on blood oxygenation. *Proc Natl Acad Sci USA* 1990;87:9868–9872.
2. Seto E, Sela G, McIlroy WE, Black SE, Staines WR, Bronskill MJ, McIntosh AR, Graham SJ. Quantifying head motion associated with fMRI motor tasks. *NeuroImage* 2000;14:284–297.
3. Woods RP, Cheery SR, Mazziota JC. Rapid automated algorithm for aligning and reslicing PET images. *J Comput Assist Tomogr* 1992;16:620–633.
4. Friston KJ, Ashburner J, Frith CD, Poline J-B, Heather JD, Frackowiak RSJ. Spatial registration and normalization of images. *Hum Brain Mapp* 1995;3:165–189.
5. Hajnal JV, Saeed N, Soar EJ, Oatridge A, Young IR, Bydder GM. A registration and interpolation procedure for subvoxel matching of serially acquired MR images. *J Comput Assist Tomogr* 1995;19:289–296.
6. Welch EB, Manduca A, Grimm RC, Ward HA, Jack CRJ. Spherical navigator echoes for full 3D rigid body motion measurement in MRI. *Magn Reson Med* 2002;1:32–41.
7. Ciulla C, Deek FP. Performance assessment of an algorithm for the alignment of fMRI time series. *Brain Topogr* 2002;14:313–332.
8. Derbyshire JA, Wright GA, Henkelman RM, Hinks RS. Dynamic scan-plane tracking using MR position monitoring. *J Magn Reson Imaging* 1998;8:924–932.
9. Mathiak K, Posse S. Evaluation of motion and realignment for functional magnetic resonance imaging in real time. *Magn Reson Med* 2001;45:167–171.
10. Thesen S, Heid O, Mueller E, Schad LR. Prospective acquisition correction for head motion with image-based tracking for real-time fMRI. *Magn Reson Med* 2000;44:457–465.
11. Cox RW. AFNI. software for analysis and visualization of functional magnetic resonance neuroimages. *Comput Biomed Res* 1996;29:162–173.
12. Cox RW, Jesmanowicz A. Real-time 3D image registration for functional MRI. *Magn Reson Med* 1999;42:1014–1018.
13. Glossop N, Hu R, Dix G, Behairy Y. Registration methods for percutaneous image guided spine surgery. Paris, France, 1999. p 746–755.
14. Horn BKP. Closed-form solution of absolute orientation using unit quaternions. *J Opt Soc Am A* 1987;4:629–642.
15. Brandt T, Dieterich M. The vestibular cortex. Its locations, functions, and disorders. *Ann NY Acad Sci* 1999;871:293–312.
16. Glover GH, Lai S. Self-navigated spiral fMRI: interleaved versus single-shot. *Magn Reson Med* 1998;39:361–368.
17. Bernstein MA, Zhou XJ, Polzin JA, King KF, Ganin A, Pelc NJ, Glover GH. Concomitant gradient terms in phase contrast MR: analysis and correction. *Magn Reson Med* 1998;39:300–308.

- AQ: 1**
- AQ: 2**
18. Menon RS, Kim SG. Spatial and temporal limits in cognitive neuroimaging with fMRI. *Trends Cogn Sci* 1999;3:207–216.
 19. Menon RS, Luknowsky DC, Gati JS. Mental chronometry using latency-resolved functional MRI. *Proc Natl Acad Sci USA* 1998;95:10902–10907.
 20. Eviator H, Schattka B, Sharp JC, Rendall J, Alexander ME. Real-time head motion detection for fMRI. In: *Proceedings of the 7th Annual Meeting of ISMRM, Philadelphia*; 1999. p 269.
 21. Nevo E, Roth A, Hushek S. An electromagnetic 3D locator system for use in MR scanners. In: *Proceedings of the 10th Annual Meeting of ISMRM, Honolulu*, 2002. p 334.
 22. Fitzpatrick JM, West JW, Maurer CRJ. Predicting error in rigid-body point-based registration. *IEEE Trans Med Imaging* 1998;17:694–702.
 23. Tregellas RJ, Tanabe JL, Miller DE, Freedman R. Monitoring eye movements during fMRI tasks with echo planar images. *Hum Brain Mapp* 2002;17:237–243.
 24. Freire L, Mangin JF. Motion correction algorithms may create spurious brain activations in the absence of subject motion. *NeuroImage* 2001;14:709–722.
 25. Hutton C, Bork A, Josephs O, Deichmann R, Ashburner J, Turner R. Image distortion correction in fMRI: a quantitative evaluation. *Neuroimage* 2002;16:217–240.
 26. Petit L, Beauchamp MS. Neural basis of visually guided head movements studied with fMRI. *Neurophysiology* 2003;89:2516–2527.
 27. Poncelet BP, Wedeen VJ, Weisskoff RM, Cohen MS. Brain parenchyma motion: measurement with cine echo-planar MR imaging. *Radiology* 1992;185:645–651.
 28. Kim B, Boes JL, Bland PH, Chenevert TL, Meyer CR. Motion correction in fMRI via registration of individual slices into an anatomical volume. *Magn Reson Med* 1999;41:964–972.
 29. Zaitsev M, Dold C, Hennig J, Speck O. Prospective real-time slice-by-slice 3D motion correction for epi using an external optical motion tracking system. In: *Proceedings of the 12th Annual Meeting of ISMRM, Kyoto, Japan*, 2004. p 517.
 30. Thulborn KR. Visual feedback to stabilize head position for fMRI. *Magn Reson Med* 1999;41:1039–1043.
- AQ: 3**



Author Proof

AQ1: ISMRM meeting as meant?

AQ2: ISMRM meeting as meant?

AQ3: ISMRM meeting as meant?



Author Proof